

NASA TECHNICAL NOTE

NASA TN D-2281



NASA TN D-2281

2.1  
COPY: RETURN TO  
AFWL (WLL—)  
KIRTLAND AFB, N MEX



# RESEARCH ON RESISTANCE-HEATED HYDROGEN THRUSTORS

*by John R. Jack, Ernie W. Spisz,  
and Paul F. Brinich*

*Lewis Research Center  
Cleveland, Ohio*



RESEARCH ON RESISTANCE-HEATED  
HYDROGEN THRUSTORS

By John R. Jack, Ernie W. Spisz,  
and Paul F. Brinich

Lewis Research Center  
Cleveland, Ohio

NATIONAL AERONAUTICS AND SPACE ADMINISTRATION

For sale by the Office of Technical Services, Department of Commerce,  
Washington, D.C. 20230 -- Price \$0.75

## RESEARCH ON RESISTANCE-HEATED

### HYDROGEN THRUSTORS

by John R. Jack, Ernie W. Spisz,  
and Paul F. Brinich

Lewis Research Center

### SUMMARY

The research effort on resistance-heated hydrogen thrustors is discussed. Experimental performance data are presented for propellant flow rates varying from  $2.5 \times 10^{-4}$  to  $10^{-3}$  pound per second and for electrical input powers ranging from 0 to 38 kilowatts. Results for both tubular- and wire-coil-heat-exchanger thrustors are included.

The efficiency of the tubular-heat-exchanger thrustors was limited because they were water cooled and had large electrical-lead losses. At an input power of 28 kilowatts and a flow rate of  $10^{-3}$  pound per second, a vacuum specific impulse of 710 seconds was achieved with an overall thrustor efficiency of 36 percent. For the same flow rate, a wire-coil thrustor produced a vacuum specific impulse of 664 seconds with an overall efficiency of 59 percent.

Preliminary performance data obtained from wire-coil-heat-exchanger thrustors operated at a 6-kilowatt input power indicated that propellant leakage, radiant heat losses, and small nozzle area ratio contributed to a low overall thrustor efficiency. The propellant temperatures achieved at the 6-kilowatt power level ( $\sim 4500^\circ \text{R}$ ) were higher than those obtained from any other unit so that the vacuum specific impulses of the order of 1000 seconds appear to be definitely within the performance capabilities of a resistance-heated hydrogen thrustor.

### INTRODUCTION

This report presents a compilation of two papers (refs. 1 and 2) and the latest results obtained from the continuing research effort at the Lewis Research Center on resistance-heated hydrogen thrustors. The concept of utilizing an electrically heated tungsten heat exchanger to heat a propellant to stagnation temperatures of the order of  $5000^\circ \text{R}$  has been under investigation since early 1959 (ref. 3). Hydrogen has been used exclusively as the propellant because of its capability of achieving vacuum specific impulses of the order of 1000 seconds at this temperature level.

The resistance-heating approach for generating high-temperature gases to

produce thrust is receiving attention because of the following potentially attractive characteristics: (1) high efficiency, (2) ability to utilize alternating- or direct-current power over a wide range of voltage, (3) high reliability, (4) long operating life, (5) starting and restarting ease, and (6) operating flexibility. A major disadvantage of this heating approach is that the propellant temperature is inherently limited by the melting temperature of the heater-element material. For a heat-exchanger material such as tungsten, this corresponds to a maximum vacuum specific impulse of the order of 1100 seconds.

The research effort reported herein was undertaken to investigate the propulsion characteristics of two design approaches to the resistance-heated hydrogen thruster. One thruster utilized a low-resistance tungsten-tube heat exchanger and was water cooled, whereas the other used a high-resistance wire-coil heat exchanger and was radiation cooled.

#### SYMBOLS

A	nozzle flow area, sq in.
A*	nozzle throat area, sq in.
$A_e/A^*$	nozzle area ratio
d*	nozzle throat diameter, in.
F	measured thrust, lb
H	enthalpy, Btu/lb
I	specific impulse, sec
$I_{vac}$	vacuum specific impulse, $\frac{F + p_a A_e}{\dot{W}}$ , sec
M	Mach number
P	power
$P_E$	electrical input power, kw
$P_i$	initial power, power in propellant prior to heat addition, kw
$P_p$	total propellant power after heat addition, that is, electrical power plus initial power $P_i$ minus power lost because of cooling, kw
$P_p/P_E$	heating efficiency
p	pressure, lb/sq in. or atm

$P_{0,1}$  stagnation pressure, lb/sq in.  
 $P_{0,2}$  probe stagnation pressure, lb/sq in.  
 $r$  radial coordinate, ft  
 $T$  temperature  
 $v$  propellant velocity, ft/sec  
 $\dot{w}$  propellant flow rate, lb/sec  
 $\gamma$  specific-heat ratio  
 $\eta$  overall thruster efficiency  
 $\rho$  density, lb/cu ft  
 $\sigma$  static sublimation rate of tungsten in hydrogen atmosphere,  
 lb/(sq in.)(sec)  
 $\psi$  Mach number parameter

Subscripts:

$a$  ambient conditions  
 $e$  nozzle exit conditions  
 $f$  frozen conditions  
 $vac$  vacuum  
 $w$  wire  
 $0$  stagnation conditions  
 $1$  conditions before probe normal shock  
 $2$  conditions after probe normal shock

Superscript:

$(*)$  throat

## THRUSTER PERFORMANCE AND LIFETIME CONSIDERATIONS

To be useful for space propulsion application, electrothermal thrusters should have the following performance characteristics: (1) a vacuum specific impulse greater than 900 seconds, (2) an overall efficiency of at least 70 percent, and (3) operating lifetimes greater than 20 days. Figure 1

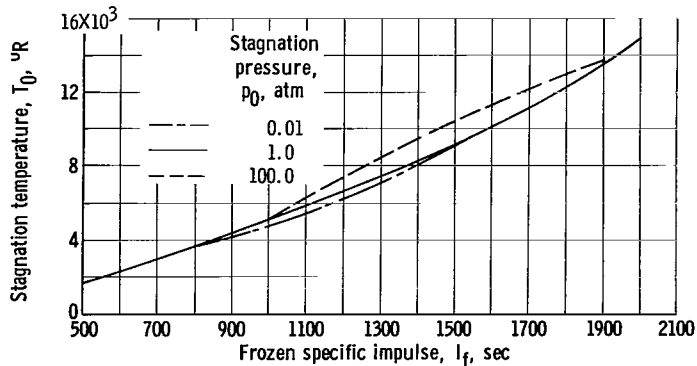


Figure 1. - Effect of pressure on hydrogen stagnation temperature.

consequently, on overall thruster efficiency. The effect of stagnation pressure on frozen specific impulse and frozen flow efficiency (the ratio of power available for thrust to the total power in the propellant  $(P_p - P_f)/P_p$ ) is shown in figure 2 for a stagnation temperature of  $5040^\circ \text{R}$ . The data of reference 4 were used to prepare figure 2. It is to be noted, for example, that to achieve the aforementioned performance characteristics requires a stagnation pressure greater than 0.2 atmosphere. The values in figure 2 represent the maximum frozen flow performance attainable with an infinite nozzle area ratio (or pressure ratio) and with regenerative cooling.

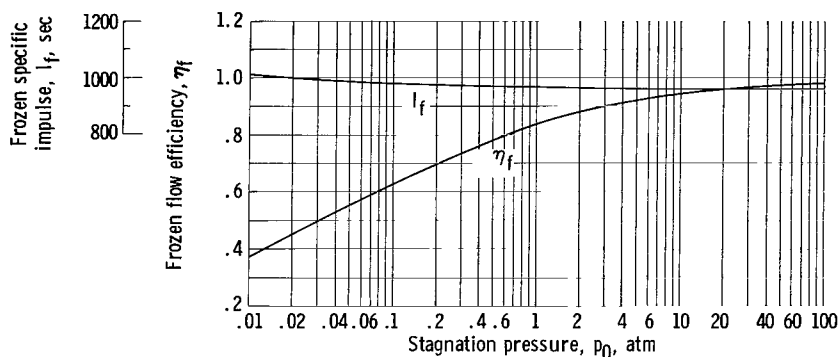


Figure 2. - Variation of hydrogen frozen flow efficiency and specific impulse with stagnation pressure. Stagnation temperature,  $5040^\circ \text{R}$ .

ing. One other major loss that must be considered before a reasonable maximum overall thruster efficiency can be ascertained is that due to finite flow expansion (finite nozzle pressure ratio and area ratio). This expansion loss is defined by a nozzle expansion efficiency that is the ratio of the thrust power in the exiting jet to the total power available for thrust. The product of the frozen flow and expansion efficiencies may be considered as a reasonable upper limit on overall thruster efficiency provided that the thruster is regeneratively cooled and that no hydrogen recombination occurs in the nozzle flow. This overall efficiency is shown in figure 3 as a function of vacuum specific impulse, stagnation temperature, and nozzle area ratio for a hydrogen electrothermal thruster operating at a stagnation pressure of 1 atmosphere. The pressure chosen here is arbitrary but does provide the desired specific impulse and an efficiency greater than 70 percent. The numerical values used in preparing figure 3 were obtained from the one-dimensional performance calculations of reference 5.

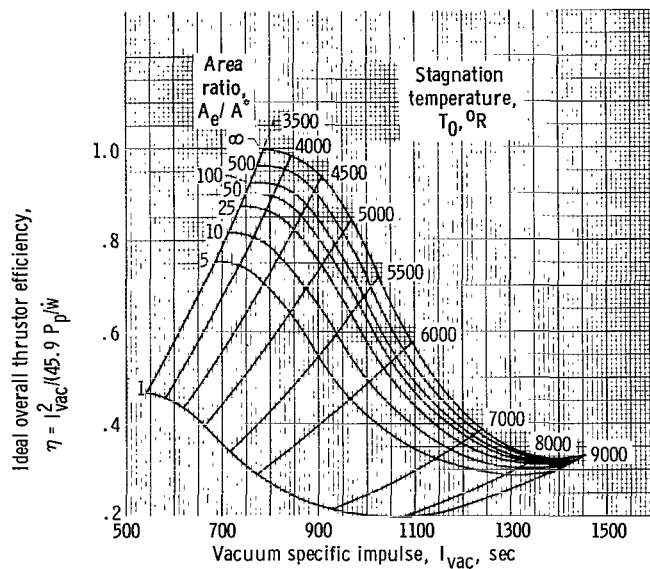


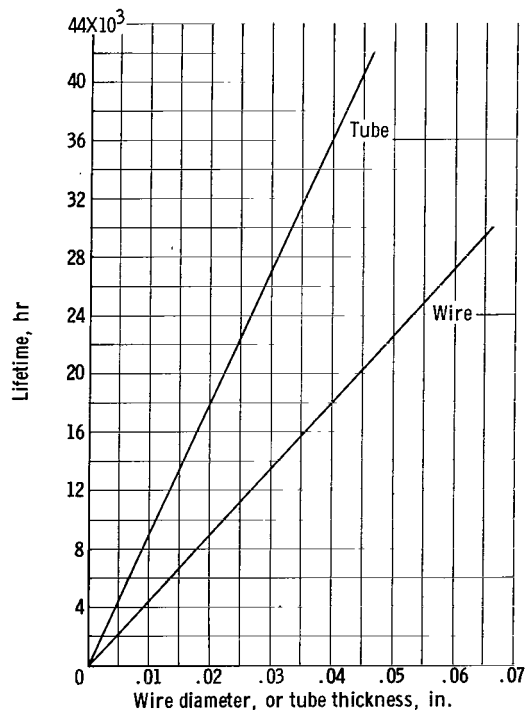
Figure 3. - Frozen flow performance characteristics of hydrogen. Stagnation pressure, 1 atmosphere; reference temperature, 0° R.

With the aid of figure 3, some conclusions regarding the operation of an electrothermal thruster in a vacuum facility and in space may be made. In the Lewis facility used for the present tests, area ratios as large as 10 can be investigated at stagnation pressures of the order of 1 atmosphere without overexpansion. With these conditions, the maximum overall thruster efficiency that can be expected is about 70 percent and the corresponding vacuum specific impulse is 875 seconds for a temperature of 5000° R. Extrapolating this operating point to space conditions, where the nozzle area ratio can become large, for example, 500, permits the overall efficiency to approach 82 percent and

the specific impulse to approach 950 seconds.

A final important factor to be considered for the resistance-heated hydrogen thruster is its operational lifetime. Based on the preceding analysis, the propellant temperature required to obtain the desired performance is of the order of 5000° R, and, consequently, the heat-exchanger material must be capable of withstanding this temperature. For satisfactory operation at this temperature level, the heat-exchanger material must be tungsten or perhaps one of the refractory carbides. Based on the high temperature required to provide the desired thruster performance, it is reasonable to expect that an indication of operational lifetimes could be obtained by considering the amount of heat-exchanger material lost by sublimation. Therefore, operational lifetimes, defined as the time required to lose 10 percent of the original weight by sublimation, have been calculated by using the static, hydrogen-atmosphere, sublimation rates presented in reference 6. The practical life of a wire filament ends when its cross section decreases by about 10 percent (or a 10-percent loss in weight), because burnout usually occurs soon thereafter (ref. 7). The lifetimes evaluated in this manner should be fairly realistic except for the variation of lifetime with pressure (or flow). Based on the preliminary results of reference 6 obtained at 5400° R, the sublimation rates with hydrogen flow are considerably higher than the static rates for pressures greater than 2 atmospheres. At pressures below this value, the two rates are approximately equal.

Figure 4(a) shows the variation of lifetime for a temperature of 5040° R and a pressure of 1 atmosphere for the two tungsten heat-exchanger configurations adapted for the research reported herein - a wire coil and a thin-walled



(a) Wire temperature, 5040° R; stagnation pressure, 1 atmosphere; static sublimation rate of tungsten in hydrogen atmosphere,  $\sigma$ ,  $1.06 \times 10^{-11}$  pound per square inch per second.

Figure 4. - Lifetime characteristics of tungsten tubes and wires in a hydrogen atmosphere.

cylindrical tube. For identical tube thickness and wire diameter, the tube lifetime is twice the wire lifetime because its ratio of volume to area per unit length is twice that for the wire. If a comparison is made for the tube thickness currently being used (0.010 in.) and the wire diameter being used (0.060 in.), however, the wire lifetime is approximately three times that obtained for the tube configuration. Figures 4(b) and (c) present the lifetime variation with temperature and pressure. The important things to note are that an increase in temperature reduces the lifetime significantly, whereas an increase in pressure increases the lifetime significantly. The latter lifetime variation at pressures greater than 2 atmospheres may not be realistic, however, and should be viewed in light of the comments made previously concerning the effect of a hydrogen flow on the sublimation rates.

The propellant stagnation conditions chosen for the experimental thrusters were a pressure of approximately 1 atmosphere and a temperature of about 5000° R. From the preceding discussion, it appears that these operating conditions will yield

the desired vacuum specific impulse, overall thruster efficiency, and operational lifetime.

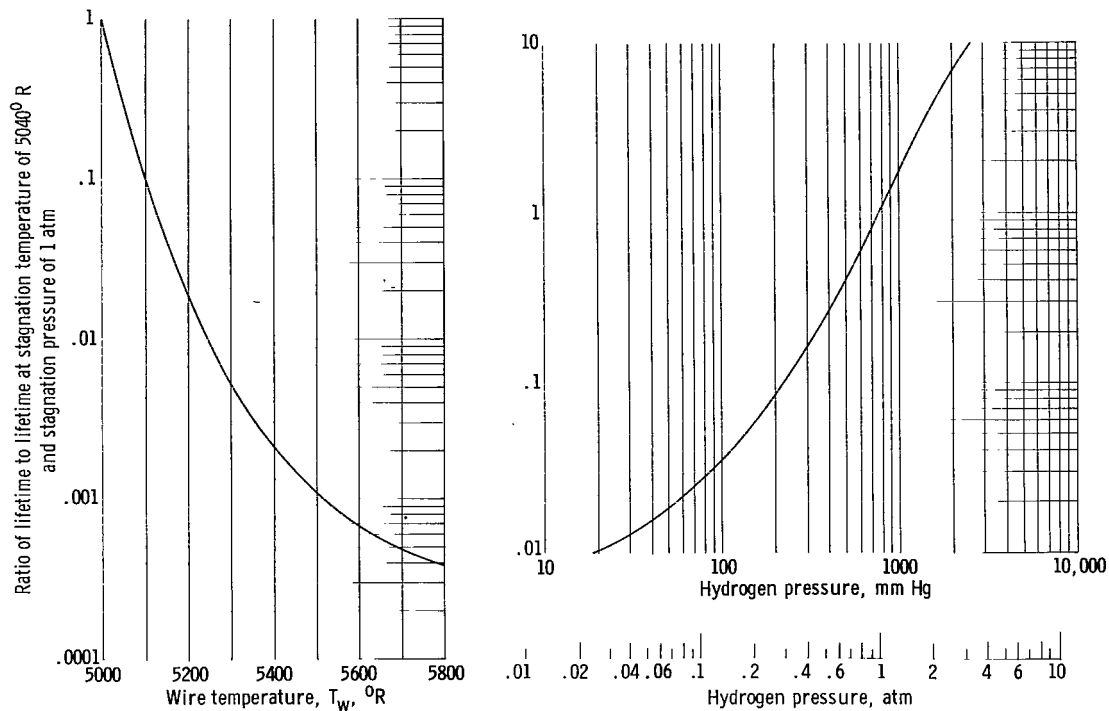
## APPARATUS

### Description of Thrusters

Two basic types of thrusters were investigated; the first was a water-cooled design with a tubular heat exchanger, which operated at currents in excess of 2000 amperes, while the other was a radiation-cooled design with a wire-coil heat exchanger, which operated at currents less than 200 amperes.

Two versions of the tubular heat-exchanger thruster, designated T-1 and T-2, were investigated at a propellant flow rate of  $10^{-3}$  pound per second. Heat-exchanger T-1 had a radiation-cooled molybdenum nozzle, heat-exchanger T-2 had a water-cooled graphite nozzle. The details of these models are shown in figure 5. Basically, the heater design consisted of a tubular heater with two tungsten radiation shields that provided a four-pass heat-exchanger system for the propellant as it passes through the unit. The heater tube was formed of 0.010-inch tungsten sheet rolled into a 1-inch-diameter tube and electron-beam welded along the seam. The heater tube for thruster T-1 had a heated

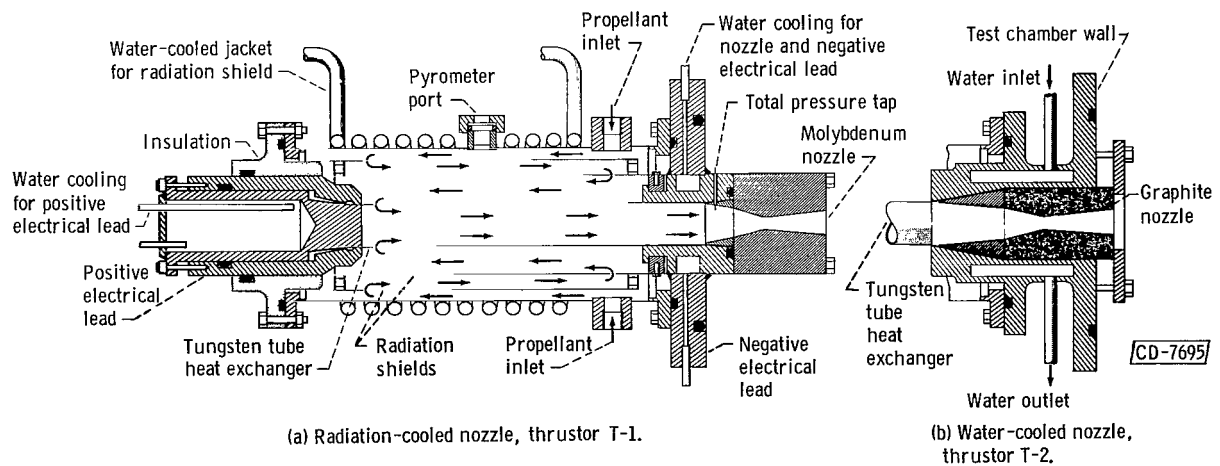




(b) Effect of temperature on lifetime.

(c) Effect of pressure on lifetime.

Figure 4. - Concluded. Lifetime characteristics of tungsten tubes and wires in a hydrogen atmosphere.



(a) Radiation-cooled nozzle, thruster T-1.

(b) Water-cooled nozzle, thruster T-2.

Figure 5. - Water-cooled tubular-heat-exchanger thruster.

length of  $6\frac{1}{2}$  inches, whereas the heated length for T-2 was 5 inches. Both tubes had small perforations on the upstream half to admit propellant into the tube for its final pass through the heater element before it entered the nozzle. Both thrusters T-1 and T-2 had nominal nozzle throat diameters of 0.214 inch and an exit- to throat- nozzle-area ratio of 5.33. In order to measure heat losses conveniently, to eliminate sealing and other design problems, and to handle the high currents, auxiliary water cooling was provided for the tube heat-exchanger units.

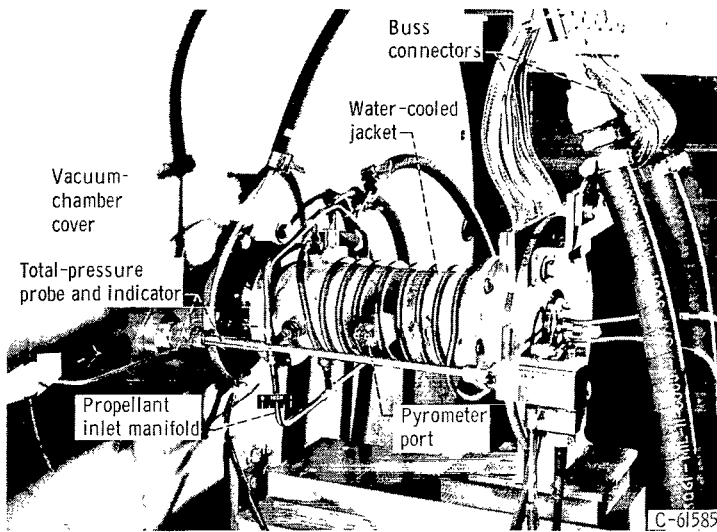
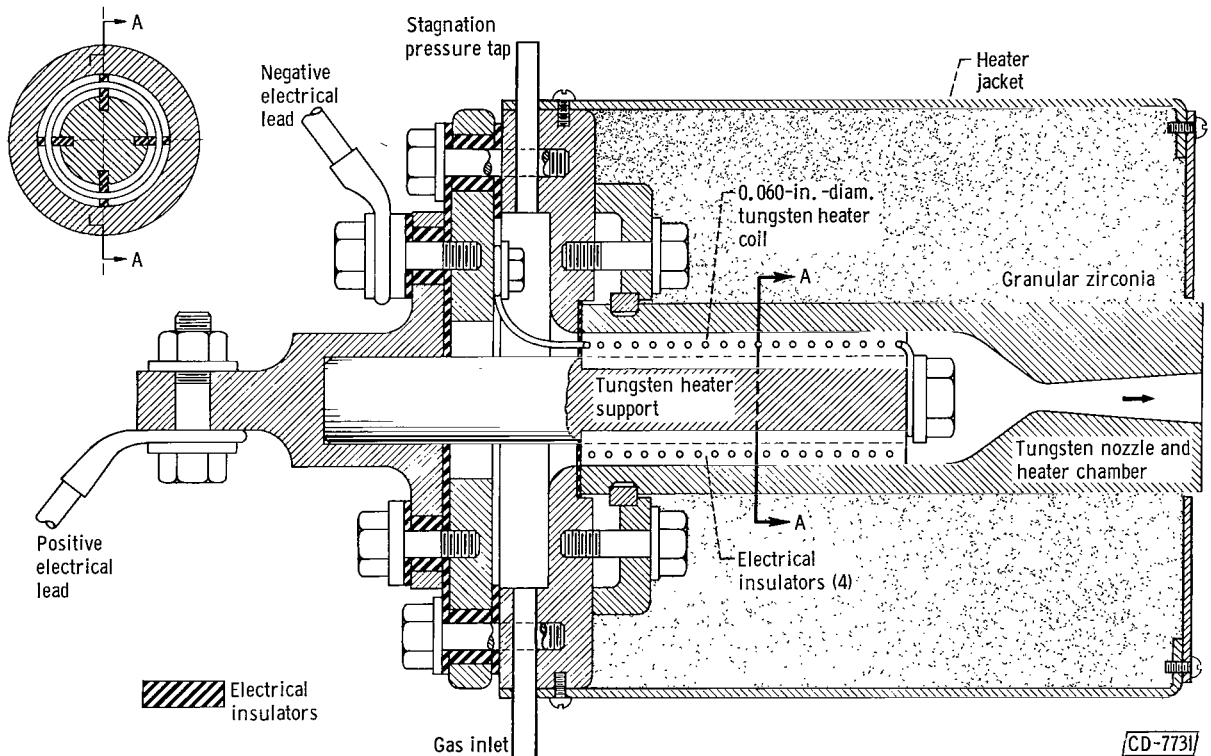


Figure 6. - Tubular-heat-exchanger thruster installed on vacuum tank.

The piping required for water cooling and the large electrical leads required to carry the high currents imposed restrictions on the method of obtaining performance data on these units, inasmuch as they could not be tested on a simple

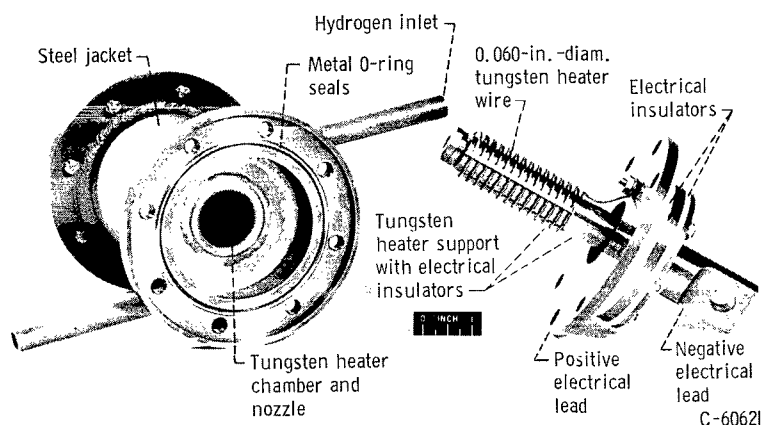


(a) Schematic diagram of thruster C-2.

Figure 7. - Radiation-cooled wire-coil-heat-exchanger thruster.

thrust platform. These units were rigidly flange-mounted to the end cover of the testing tank, as shown in figure 6.

Two coil-heat-exchanger thrusters designated C-1 and C-2 were investigated. Sketches and photographs of these are shown in figure 7. Basically, the wire-coil design consisted of the tungsten heater coil, which was supported by boron nitride spacers on a tungsten heater support. The coil was inserted into a tungsten nozzle body, which was insulated by a thick layer of granular zirconia. The heater coils for both thrusters (figs. 7(a) and (b)) were formed of 0.060-inch-diameter tungsten wire 50 inches long wound into 1-inch-diameter coils with a pitch of 0.180. The nozzle for thruster C-1 had a throat diameter of 0.206 inch and an area ratio of 5.33 and was tested with a propellant flow rate of  $10^{-3}$  pound per second.



(b) Photograph of thruster C-1.

Figure 7. - Concluded. Radiation-cooled wire-coil-heat-exchanger thruster.

Thruster C-2 differed from C-1 only in that the nozzle area ratio was 2.0 rather than 5.33 and that the propellant flow rate was varied from  $0.25 \times 10^{-3}$  to  $10^{-3}$  pound per second. Test results were obtained both with and without the insulating jacket over the heater chamber and nozzle. Detailed specifications for the four thrusters described are summarized in table I.

TABLE I. - THRUSTER SPECIFICATIONS

Thruster	Heater element			Nozzle			Operating conditions	
	Type	Material	Dimensions	Description	Throat diameter, $d^*$ , in.	Area ratio, $A_e/A^*$	Propellant flow rate, $\dot{w}$ , lb/sec	Electrical input power, $P_E$ , kW
T-1	Tube	0.010-in.-thick tungsten sheet	1-in.-diam. tube; $\frac{1}{2}$ -in. effective heated length	Radiation-cooled molybdenum	0.214	5.33	$10^{-3}$	$0 \leq P_E \leq 38$
T-2			1-in.-diam. tube; 5-in. effective heated length	Water-cooled graphite				
C-1	Wire coil	0.060-in.-diam. tungsten wire (50 in. length)	1-in.-diam. coil; pitch, 0.180 in.	Radiation-cooled tungsten	0.206	5.33	$10^{-3}$	$0 \leq P_E \leq 18$
C-2						0.210	2.0	$0.25 \times 10^{-3} \leq \dot{w} \leq 10^{-3}$

## Test Facility

The test facility used for obtaining operating performance of the thrustors consisted of a stainless-steel vacuum tank 3 feet in diameter and 6 feet in length with exhaust capabilities of maintaining a pressure of 7 to 12 millimeters of mercury for all propellant rates of interest. Direct-current power was supplied as required by motor generator sets or conversion equipment. Gaseous hydrogen was supplied by a bank of six commercial bottles through a calibrated rotameter, or choked orifice, for flow-rate metering.

The thrustors were mounted or suspended in the tank in the following manner. The tube-heated thrustors were bolted directly to the tank flange, and the propellant discharged into the tank. As discussed in the appendix, thrust was determined by centerline total-pressure measurements at the nozzle exit plane by a tungsten probe. The coil-heated thrustors were mounted on a platform that was freely suspended by four wire cables from a stationary frame inside the tank. Thrust was measured by force transducers that have a negligible displacement.

## Thrustor Instrumentation

Thrustor stagnation pressures were measured immediately upstream of the nozzle for thrustor T-1, as indicated in figure 5(a), by a pressure transducer. No pressures were measured in the thrustor with the water-cooled nozzle, T-2. Stagnation pressures in the coil-heated thrustors, C-1 and C-2, were measured in the plenum chamber, upstream of the heater elements.

Tube heater temperatures of thrustors T-1 and T-2 were obtained with a pyrometer by viewing the tube through the pyrometer port shown in figure 5(a). Temperature measurements of the molybdenum nozzle for thrustor T-1 were made with platinum-rhodium thermocouples. These measurements were used to estimate radiant heat losses from the radiation-cooled nozzle in figure 5(a).

The coil-heat-exchanger thrustors, C-1 and C-2, had six Chromel-Alumel thermocouples to measure the outer jacket temperature and three tungsten-rhenium thermocouples to measure the heater chamber and nozzle temperatures. Thermocouples were also installed on the power leads for some of the tests to assess the power lost through the electrical conductors. All thermocouple outputs were measured on self-balancing potentiometers.

## RESULTS AND DISCUSSION

Experimental results are presented for both tubular- and coil-heat-exchanger thrustors. All the thrustors investigated were designed for operation at a maximum heat-exchanger temperature of 5500° R. Hydrogen flow rates varied from  $2.5 \times 10^{-4}$  to  $10^{-3}$  pound per second, and electrical input powers ranged from 0 to 38 kilowatts. Performance is presented in terms of vacuum specific impulse,  $I_{vac}$ , which is defined as the specific impulse obtained with zero ambient pressure,  $I_{vac} = (F + P_a A_e) / \dot{w}$ . This is used to eliminate the

effect of vacuum tank pressure, which varied from 7 to 12 millimeters of mercury.

### Tubular-Heat-Exchanger Thrustors

Experimental results were obtained with thrustors T-1 and T-2 at input powers up to 38 kilowatts and gas and heat-exchanger temperatures as high as 4500° and 5000° R, respectively. The basic heat exchanger has been operated with both a radiation-cooled molybdenum nozzle (thrustor T-1) and a water-cooled graphite nozzle (thrustor T-2). The radiation-cooled nozzle was used to investigate the increased performance that could be expected because of the resulting higher heating efficiency.

Figure 8 presents vacuum specific impulse as a function of electrical

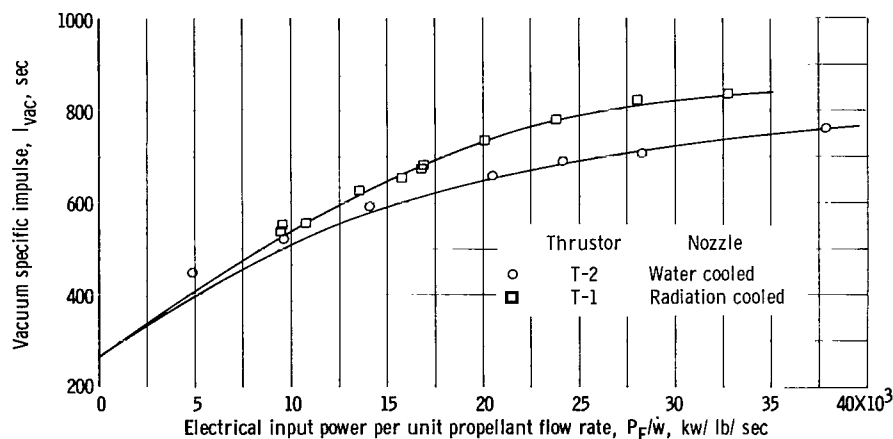


Figure 8. - Specific impulse as function of electrical input power for tubular-heat-exchanger thruster. Hydrogen flow rate,  $10^{-3}$  pound per second; nozzle area ratio, 5.33; nozzle throat diameter, 0.214 inch.

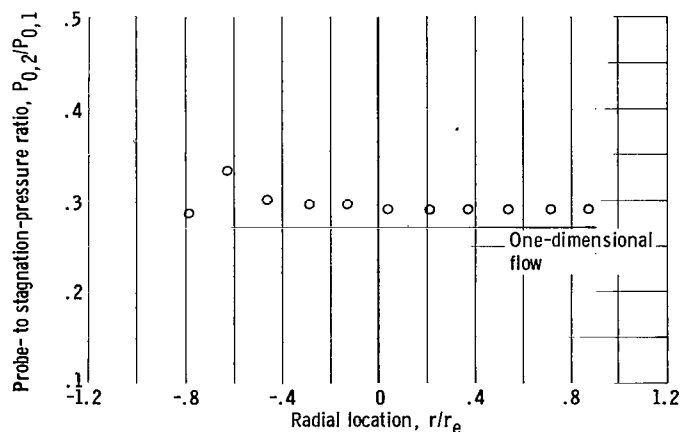


Figure 9. - Jet total-pressure profile.

input power per unit propellant flow rate. The vacuum specific impulse is based on the measured flow rate and thrust as evaluated from centerline total-pressure-probe measurements (see the appendix). Use of centerline measurements is partly justified by a typical cold jet survey shown in figure 9, which shows an exceptionally flat total-pressure profile. A comparison of the performance data for the water-cooled and radiation-cooled nozzles indicates the expected better performance for the radiation-cooled design at a

given electrical input power. At the approximate design operating point of 28 kilowatts, the vacuum specific impulses obtained from probe measurements are 710 and 825 seconds for the water-cooled and radiation-cooled nozzles, respectively, which correspond to overall thruster efficiencies of 36 and 50 percent. The overall thruster efficiency quoted herein is defined as

$$\eta = \frac{\dot{w} I_{vac}^2}{45.9(P_E + P_i)}$$

and is the ratio of effective jet power to total input power.

The performance data obtained from probe measurements are compared in figure 10 with calculated values for the propellant power, nozzle area ratio,

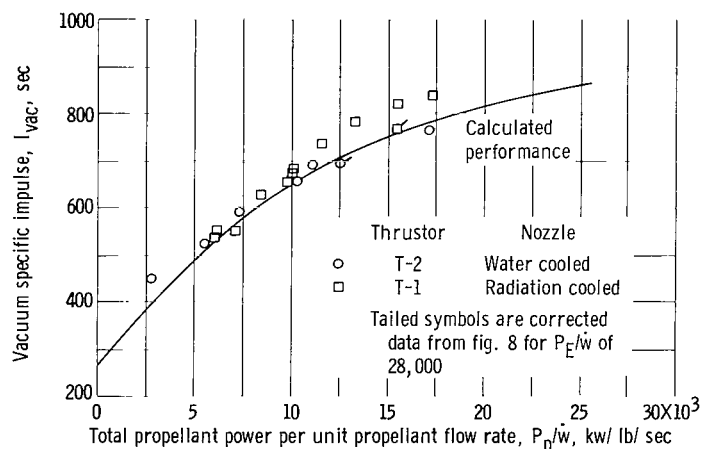


Figure 10. - Specific impulse as function of total propellant power for tubular heat-exchanger thruster. Hydrogen flow rate,  $10^{-3}$  pound per second; nozzle area ratio, 5.33; nozzle throat diameter 0.214 inch; tank pressure, 10 millimeters of mercury.

and propellant flow rate. The calculated values are based on a frozen one-dimensional, isentropic, expansion process. Above a value of gas power per unit propellant flow rate ( $P_E/\dot{w}$ ) of 10,000, the data obtained with the radiation-cooled nozzle deviate somewhat from the calculated performance; however, the data obtained with the water-cooled nozzle correlate with the calculated performance. This discrepancy exists because of the approximations made in determining thrust by the probe technique. For example, correcting the data points at a value of the electrical input power per unit propellant flow rate ( $P_E/\dot{w}$ ) of 28,000 in figure 8 for both the approximation made in the equation used for determining thrust and the effect of boundary layer on the exit area yields data points (tailed symbols in fig. 10) that agree well with theory (see the appendix for details). Thus, it appears that the complete thrust equation and the effect of boundary layer on nozzle exit area must be used, particularly for cases where the nozzle operates at a high wall temperature (radiation-cooled nozzle). Now, if the overall thruster efficiency is computed for the data points at  $P_E/\dot{w} = 28,000$  (fig. 8), efficiencies of 43 and 35 percent are obtained for thrusters T-1 and T-2, respectively. This difference in overall efficiency is just about what would be expected based on the difference in heating efficiencies obtained for the two thrusters. The substantially good agreement between the measured data and the computed curve over the entire power range indicates, in general, the validity of the one-dimensional isentropic flow assumption and of the probe technique used to determine thrust.

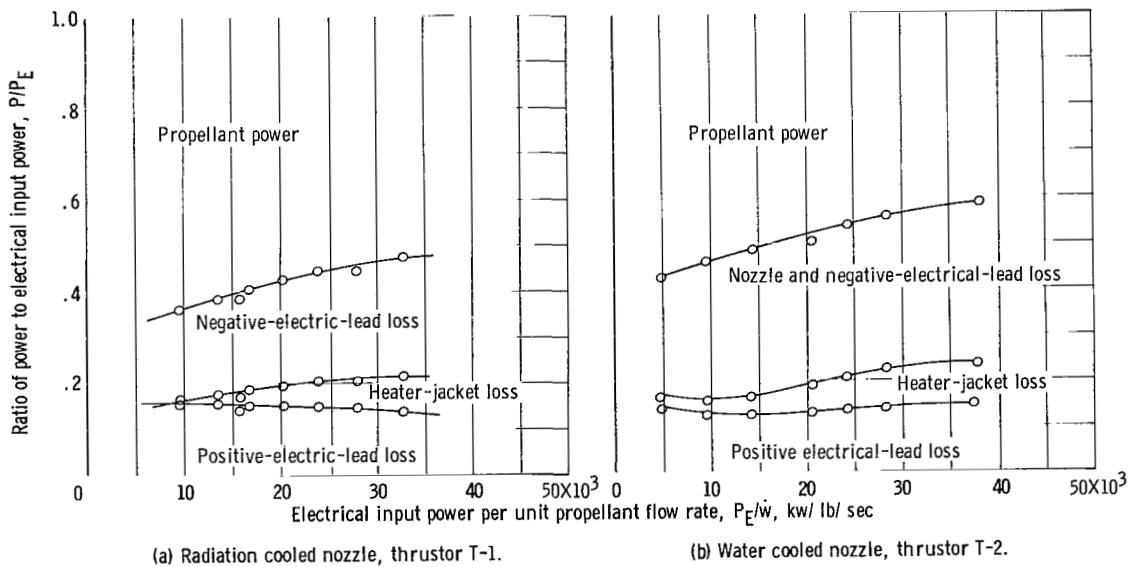


Figure 11. - Thrustor power balance. Hydrogen flow rate,  $10^{-3}$  pound per second.

A power balance, obtained by separate cooling loops for both thruster configurations (see fig. 5) is presented in figure 11 for a propellant flow rate of  $10^{-3}$  pound per second. There are several interesting facts to be obtained from this figure. First, note that at the highest input power or highest heat-exchanger temperature the loss to the heater jacket is only of the order of 9 percent. Thus, the two radiation shields and the regenerative cooling of them are fairly effective. This loss could be reduced substantially by the introduction of one more radiation shield and by making the cooling passageways more efficient. Next, the losses associated with the electrical connections are quite large. For example, for the thruster with the water-cooled nozzle at an input power of 30 kilowatts, it is estimated, based on the nozzle heat-transfer calculations presented in reference 3, that the total heat loss attributed to the electrical leads is roughly 11 kilowatts (6.6 kw from the negative lead and 4.4 kw from the positive lead), whereas the heat loss attributed to the nozzle is about 3.6 kilowatts. This indicates that the ohmic heat loss is high so that it would be desirable to design a high-voltage, low-current engine. All the losses shown in figure 11 contribute to the low heating efficiencies (ratios of propellant power to input power) presented in figure 12 for the two nozzle configurations. At an input power level of

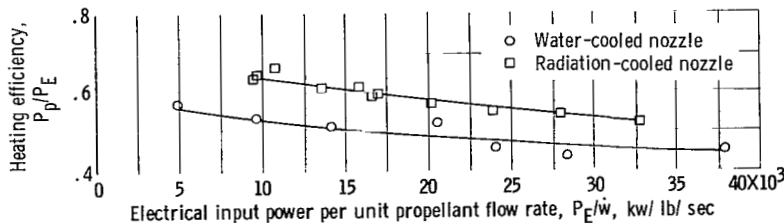


Figure 12. - Experimental heating efficiency of tubular-heat-exchanger thruster. Hydrogen flow rate,  $10^{-3}$  pound per second.

30 kilowatts, the thruster with the water-cooled nozzle has a heating efficiency of 43 percent, whereas the efficiency obtained with the radiation-cooled nozzle is 53 percent.

Based on the experience gained thus far, tube

heat exchangers appear capable of providing the desired propellant temperatures of 5000° R. If the efficiency is to be increased to a reasonably high level, however, a completely radiation-cooled or regeneratively cooled design is necessary. This creates several difficult design problems, such as electrical lead loss, conduction losses, sealing problems, and thermal expansion problems. At this time, the wire-coil thruster appears to offer better performance in terms of efficiency with considerably less severe design problems. Therefore, most of the NASA research effort is now being devoted to the wire-coil thruster.

### Coil-Heat-Exchanger Thrusters

Thruster C-1. - This unit was the first attempt at a coil-heat-exchanger design with a radiation-cooled thruster body. Figure 13 presents a comparison

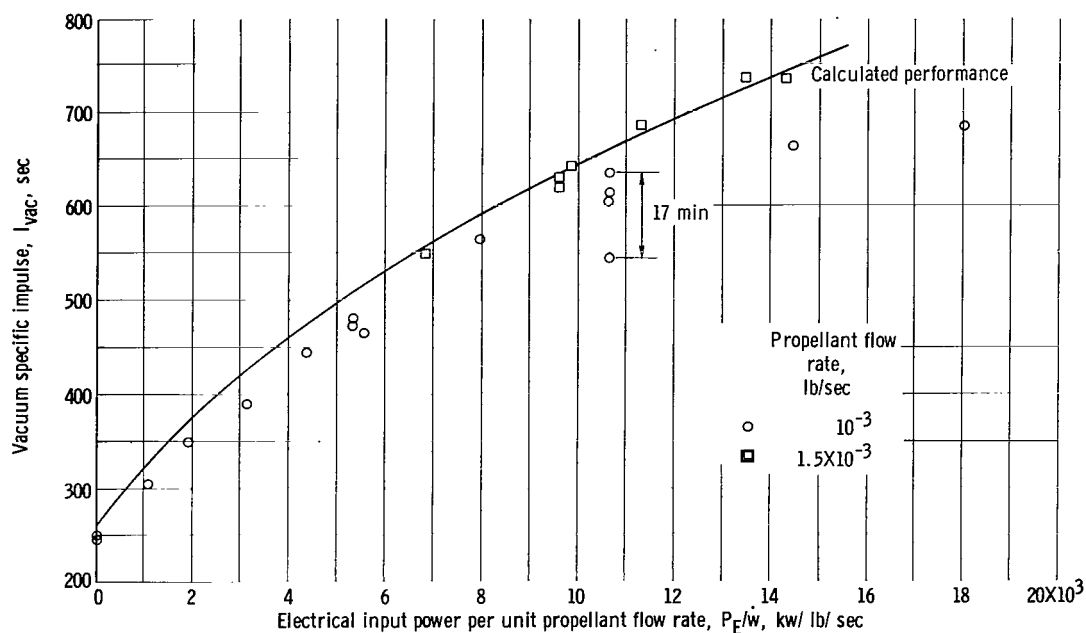


Figure 13. - Performance characteristics of coil-heat-exchanger thruster C-1. Nozzle throat diameter, 0.206 inch; nozzle area ratio, 5.33.

of the experimentally measured and calculated specific impulse as a function of electrical input power per unit propellant flow rate. The experimental data are based on the measured values of thrust, propellant flow rate, voltage, and current. As for the tube-type thrusters, the calculated curve is based on a one-dimensional, isentropic, frozen flow expansion process for the corresponding nozzle geometry. In this comparison, no allowance is made for the radiant heat losses from the surface of the unit. Calculations from surface temperature measurements indicated that the radiant heat loss was less than 3 percent of the input power.

To illustrate the level of performance achieved by thruster C-1, its performance will be compared to that for thruster T-1 for an identical propel-



lant flow rate of  $10^{-3}$  pound per second and an input power level of approximately 14 kilowatts. For these conditions, the vacuum specific impulse is 664 seconds and the efficiency is 59 percent for thruster C-1 compared with a specific impulse of 591 seconds and an efficiency of 47 percent for T-2. The maximum performance point achieved with unit C-1 was obtained with a flow rate of  $1.54 \times 10^{-3}$  pound per second and produced a specific impulse of 735 seconds and an overall efficiency of 76 percent. This comparatively high efficiency at a reasonable specific impulse is indicative of the performance attainable by resistance-heated units of this design if the heat losses are negligible.

Because this thruster was radiation cooled and had a large heat capacity, it was necessary to wait a considerable period of time to achieve thermal equilibrium. The time variation of the performance at a given input power level is shown in figure 13 at a  $P_E/\dot{w}$  of 10,600. Seventeen minutes were required to approach equilibrium, as indicated by temperature measurements on the outer surface of the insulation. During this period, the vacuum specific impulse increased from 534 to 634 seconds. As a result of this effect, the input power level was maintained constant for a period of time ranging from 5 to 20 minutes, so that accurate equilibrium data could be recorded.

At the design propellant flow rate of  $10^{-3}$  pound per second, a deviation of the measured performance from the

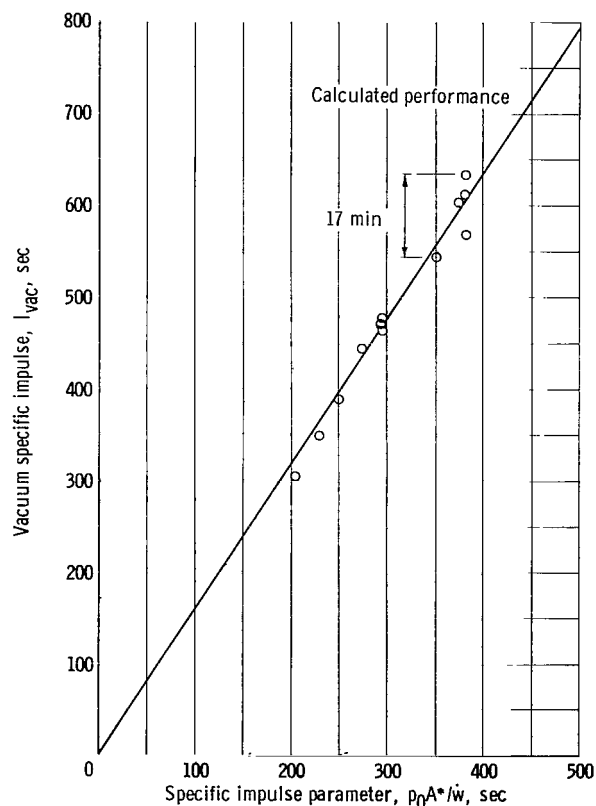


Figure 14. - Correlation of vacuum specific impulse with specific impulse parameter for coil-heat-exchanger thruster C-1. Nozzle throat diameter, 0.206 inch; nozzle area ratio, 5.33.

of the measured performance from the calculated curve is indicated at enthalpies greater than 10,000 kilowatts per pound per second (fig. 13). This deviation was caused by propellant leakage through the tungsten - stainless-steel brazed joint at the front flange, which opened because of excessive component temperatures. Improving the cooling in this area by increasing the propellant flow rate to  $1.54 \times 10^{-3}$  pound per second reduced the joint temperature and eliminated the leakage, as is indicated by the good agreement shown in figure 13 throughout the input power range. The deviation from the calculated performance was additionally verified as a leakage problem by the correlation of the data presented in figure 14, which shows a correlation of measured performance data with specific impulse parameter  $p_0 A^* / \dot{w}$ . The theoretical curve was obtained from the conventional isentropic thrust equation for zero ambient pressure presented in reference 8:

$$I_{vac} = \frac{F_{vac}}{\dot{w}} = \frac{p_0 A^*}{\dot{w}} \left[ \gamma \sqrt{\frac{2}{\gamma-1} \left( \frac{2}{\gamma+1} \right)^{\gamma+1/\gamma-1}} \sqrt{1 - \left( \frac{p_e}{p_0} \right)^{\gamma-1/\gamma}} + \frac{A_e}{A^*} \left( \frac{p_e}{p_0} \right) \right]$$

This equation with  $\gamma = 1.4$  accurately predicts experimental results for temperatures up to 5000° R and stagnation pressures above 1/2 atmosphere. The experimental correlation utilizes the measured thrust, chamber pressure, propellant flow rate, and nozzle throat diameter. Because of the normalizing effect of the propellant flow rate, the correlation is independent of the flow rate and provides an accurate comparison between measured specific impulse and chamber pressure regardless of the propellant flow rate, provided that the expansion is isentropic. As can be seen in figure 14, all the experimental data for thruster C-1 agree well with the calculated curve over the complete range of the specific-impulse parameter. This good correlation with theory confirms the isentropic expansion assumption and indicates that the measured thrust and chamber pressure correspond. Since the heat loss calculation confirms the adiabatic assumption, the deviation from theory noted in figure 13 must be caused by an incorrect propellant flow rate; that is, leakage must exist in the unit for  $P_E/\dot{w}$  greater than 10,000.

Based on measured specific impulse and/or stagnation pressure, the maximum gas temperature achieved with thruster C-1 at the design propellant flow rate of  $10^{-3}$  pound per second was 4000° R, while at  $1.54 \times 10^{-3}$  pound per second it was 3800° R. Failure to achieve higher propellant temperatures was due to burnout of the coil. Burnout normally occurred at the last two turns of the coil heat exchanger in the region of maximum propellant temperature. The design of the heater element used for this unit was relatively unsophisticated because no previous experience was available. However, the data obtained with this unit were useful for development of better design criteria.

Thruster C-2. - Thruster C-2 utilized basically the same design as C-1 except a platinum O-ring seal was used between the tungsten nozzle and the stainless-steel front flange in an attempt to eliminate the propellant leakage encountered with thruster C-1. Model C-2 was operated with the tungsten nozzle body insulated and uninsulated to determine the effect of the radiation heat loss on performance. A range of flow rates from  $2.5 \times 10^{-4}$  to  $10^{-3}$  pound per second was covered to establish the validity of the heat-exchanger analysis and the design criteria developed from the data of thruster C-1.

Figure 15 presents a comparison of the experimentally measured and calculated specific impulse as a function of electrical input power per unit propellant flow rate. This figure is similar to figure 13 for thruster C-1 except that a nozzle area ratio of 2.0 rather than 5.33 is used to establish the calculated curve.

As can be seen from figure 15, the experimental data again deviate from the calculated curve at enthalpies ( $P_E/\dot{w}$ ) greater than 10,000 kilowatts per pound per second. In order to establish whether the deviation can be attrib-

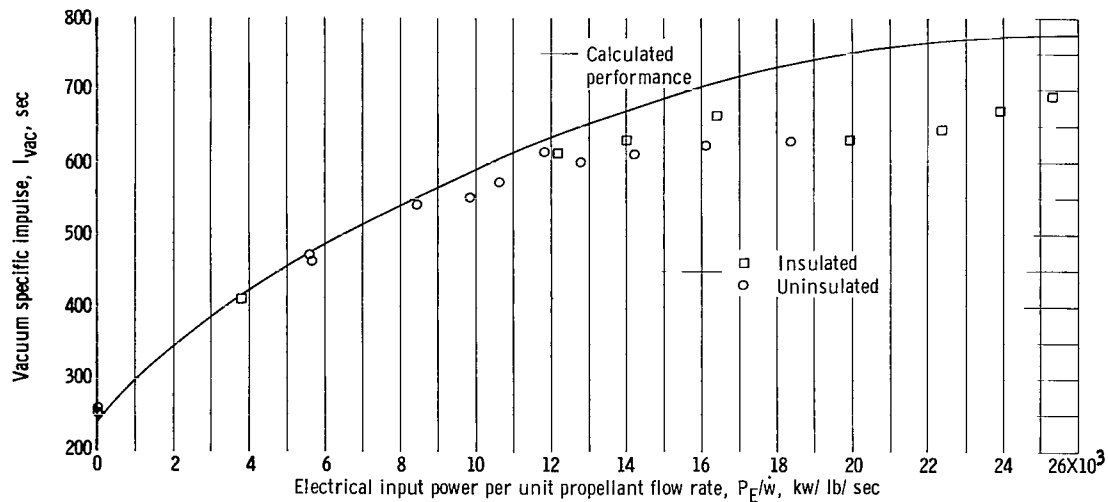


Figure 15. - Performance characteristics of coil-heat-exchanger thruster C-2. Nozzle throat diameter, 0.210 inch; nozzle area ratio, 2.0.

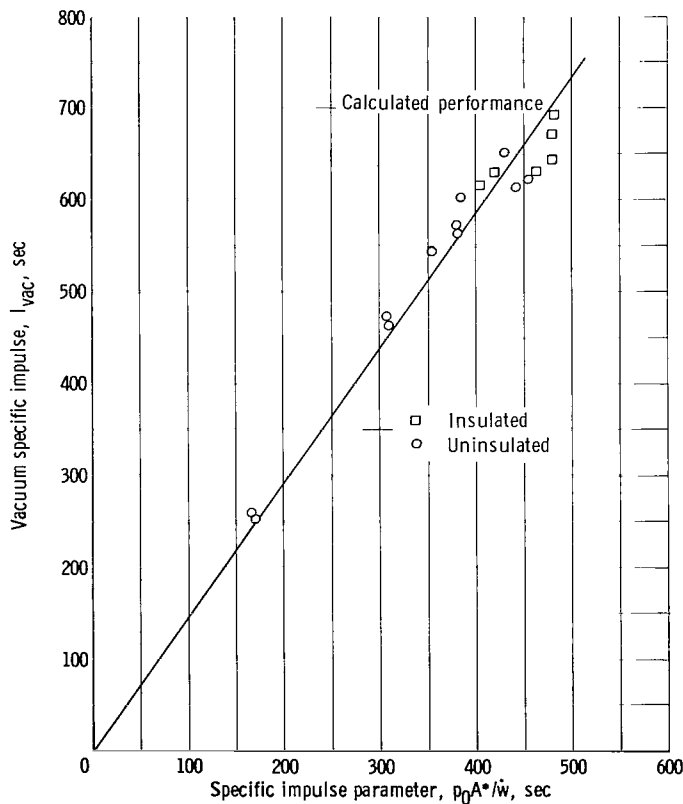


Figure 16. - Correlation of vacuum specific impulse with specific impulse parameter for coil-heat-exchanger thruster C-2; nozzle area ratio, 2.0.

uted to propellant leakage, a correlation similar to that of figure 14 was made and is presented in figure 16. This correlation shows relatively good agreement over the entire range but does not fit the theoretical curve as well as that for thruster C-1 in the region of high temperature (or high  $I_{vac}$ ). This deviation at high temperature is not due to propellant leakage since the correlation is independent of propellant flow rate. Therefore, it must be due to nonisentropic effects, namely, viscous or radiant heat losses or inaccuracy in the thrust-measuring system. The radiant heat losses associated with the low flow rates ( $2.5 \times 10^{-4}$ ) used in obtaining the high-temperature data yield heating efficiencies about 10 percent lower than those obtained with thruster C-1. In terms of specific impulse, this loss in heating efficiency lowers the specific impulse about 50 seconds, whereas the actual loss varied between 10 and 50 seconds (see fig. 16).

Thus, it appears that this deviation can be accounted for by considering both radiant heat losses and inaccuracies in the thrust-measuring system and that viscous losses are negligible for this low-area-ratio nozzle. This still does not, however, account for the 125 seconds required for the experimental data to fit the calculated performance curve of figure 15. A major portion of this difference must, therefore, again be attributed to propellant leakage at the platinum O-ring seal.

The maximum performance level achieved with thruster C-2 at an input power of 6.3 kilowatts is a vacuum specific impulse of 692 seconds at an overall efficiency of 39 percent. This is less than the maximum value of 735 seconds at 76 percent for thruster C-1. Propellant leakage, heat losses, and a small nozzle area ratio, however, degrade the performance of thruster C-2 and prevent a realistic performance comparison.

The most significant achievement for thruster C-2 that can be inferred from the stagnation pressure and/or specific impulse was the attainment of a maximum propellant temperature of  $4500^{\circ}\text{R}$  without coil burnout. This is  $500^{\circ}\text{R}$  higher than that obtained for thruster C-1. When this propellant temperature is extrapolated to a more suitable nozzle area ratio of 100 and a design stagnation pressure of 1 atmosphere, the corresponding vacuum specific impulse is 875 seconds and the possible overall thruster efficiency greater than 70 percent.

The difference in performance between the insulated and the uninsulated units was surprisingly small. This is believed to result from a tradeoff between the increased heat losses of the uninsulated unit and the propellant leakage caused by the higher temperatures of the unit components at the seal for the insulated unit. Additional effort will be required to establish completely the degree of performance improvement to be expected for a completely insulated leak-free unit.

#### SUMMARY OF RESULTS

Experimental results have been presented for two basically different types of resistance-heated hydrogen thrusters. One thruster type is a low-resistance device employing a tungsten-tube heat exchanger and is water cooled, whereas the other is a high-resistance device utilizing a tungsten-wire-coil heat exchanger and is radiation cooled. Data were obtained for four different thrusters over an input power range of 0 to 38 kilowatts for propellant flow rates of  $2.5 \times 10^{-4}$  to  $10^{-3}$  pound per second. The following experimental results were obtained:

1. For the completely water-cooled tube heat-exchanger unit at an input power level of approximately 28 kilowatts and a weight flow of  $10^{-3}$  pound per second, a corrected vacuum specific impulse of 694 seconds was achieved with an overall thruster efficiency of 35 percent. Use of a radiation-cooled nozzle with this thruster increased the vacuum specific impulse to 768 seconds and the overall efficiency 1.23 times that obtained with the water-cooled nozzle.

2. For the wire-coil unit with a nozzle area ratio of 5.33 at an input power of approximately 14 kilowatts and a weight flow of  $10^{-3}$  pound per second, a vacuum specific impulse of 664 seconds with an efficiency of 59 percent was attained. This compares with a specific impulse of 591 seconds and an efficiency of 47 percent for the water-cooled tube-heat-exchanger model at the same input power level. The higher efficiency of the wire-coil thruster was expected since the heat losses associated with it were considerably smaller than those associated with the water-cooled tube thruster. The maximum performance was achieved with this wire-coil thruster with a flow rate of  $1.54 \times 10^{-3}$  pound per second and produced a specific impulse of 735 seconds and an overall efficiency of 76 percent.

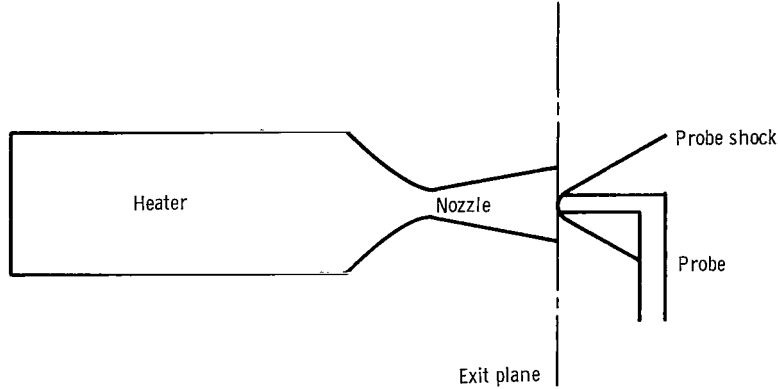
3. For the wire-coil unit with a nozzle area ratio of 2.0 at an input power of 6.3 kilowatts and a weight flow of  $2.5 \times 10^{-4}$  pound per second, a maximum specific impulse of 692 seconds with an efficiency of 39 percent was attained. This performance was not as good as that obtained for the wire-coil thruster with the higher nozzle area ratio because of propellant leakage, a small nozzle area ratio, and a larger percentage of the input power going into heat losses. The performance obtained, however, corresponds to a propellant stagnation temperature of  $4500^{\circ}$  R, which with a nozzle area ratio of 100 and a stagnation pressure of 1 atmosphere would produce a vacuum specific impulse of 875 seconds and a possible overall thruster efficiency greater than 70 percent.

Lewis Research Center

National Aeronautics and Space Administration  
Cleveland, Ohio, January 16, 1964

## APPENDIX - MEASUREMENT OF THRUST WITH PRESSURE PROBE IN JET

The thrust produced by a supersonic jet exiting into an ambient environment, whose pressure is  $p_a$ , may be found by making a pressure survey across the exit plane of the nozzle. A schematic diagram of a thruster is shown in the following sketch:



A momentum balance on the thruster yields the following general expression for the thrust:

$$\begin{aligned}
 F &= -p_a A_e + 2\pi \int_0^{r_e} (p_1 + \rho_1 v_1^2) r \, dr \\
 &= -p_a A_e + 2\pi \int_0^{r_e} (p_2 + \rho_2 v_2^2) r \, dr
 \end{aligned} \tag{A1}$$

All the terms on the right side of the equation except the ambient pressure  $p_a$  are taken to be in the nozzle exit plane. The quantities  $p$ ,  $\rho$ , and  $v$  are the static pressure, density, and velocity in the exit plane,  $r$  is the radial coordinate at the nozzle exit, and  $r_e$  and  $A_e$  are the nozzle exit radius and area, respectively. Subscripts 1 and 2 designate conditions immediately upstream and downstream of the probe shock, and the normal part of the shock is assumed to lie in the nozzle exit plane.

The flow variables under the integral sign of equation (A1) may be found in terms of the probe stagnation pressure by utilizing the binomial expansion of the equation relating the stagnation and static pressures for an isentropic flow:

$$p_{0,2} = p_2 \left( 1 + \frac{\gamma-1}{2} M_2^2 \right)^{\gamma/(\gamma-1)} \tag{A2}$$

The binomial expansion of (A2) yields

$$p_{0,2} = p_2 + \rho_2 v_2^2 \left( \frac{1}{2} + \frac{M_2^2}{8} + \dots \right) \tag{A3}$$

where  $p_{0,2}$  is the probe stagnation pressure and  $M_2$  is the Mach number immediately downstream of the normal shock. Substituting equation (A3) into equation (A1) yields for the thrust

$$F = -p_a A_e + 2\pi \int_0^{r_e} p_{0,2} [1 + \psi(M_2)] r \, dr \quad (A4)$$

where

$$\psi(M_2) = \frac{\rho_2 v_2^2}{p_{0,2}} \left( \frac{1}{2} - \frac{M_2^2}{8} - \dots \right)$$

In general, the application of equation (A4) is no easy task if the flow is nonuniform. If it can be demonstrated that the jet flow is reasonably uniform (as was demonstrated herein, see fig. 9), equation (A4) may be simplified to

$$F = [p_{0,2} - p_a + p_{0,2}\psi(M_2)] A_e$$

or

$$\frac{(F/A_e) + p_a}{p_{0,2}} = 1 + \psi(M_2) \quad (A5)$$

Furthermore, it is reasonable to evaluate equation (A5) in terms of a one-dimensional flow, so that the effect of the term  $\psi(M_2)$  may be estimated. This

has been done<sup>1</sup> for  $\gamma = 1.4$ , and the resulting thrust ratio  $\frac{F/A_e + p_a}{p_{0,2}}$  is plotted as a function of the nozzle area ratio and the stagnation-pressure ratio  $p_{0,1}/p_{0,2}$  in figure 17. Thrust ratios vary from a maximum of 1.27 at an area ratio of 1 to 1.09 at an infinite area ratio. At an area ratio of 5.33 (the nozzle area ratio employed for the tube thrusters), the thrust ratio is 1.12. Thus, since the effect of  $\psi(M_2)$  is only of the order of 10 percent for the area ratio used in the experiment and since the true state of the flow is unknown, equation (A5) was approximated to determine the thrust of the tube thrusters. The approximation used is

$$F = (p_{0,2} - p_a) A_e \quad (A6)$$

where  $A_e$  is the geometric exit area. Actually, because of the boundary-layer development in the nozzle, the total pressure measured by the probe is associated with an effective exit area that is smaller than the geometric exit

---

<sup>1</sup>The ratio  $\gamma$  has been evaluated for an assumed dissociating, perfect, diatomic gas for the experimental range of conditions with  $\gamma = (4 + 3Z)/(4 + Z)$  where  $Z$  is the compressibility factor for hydrogen. This ratio was found to vary from 1.40 to 1.42.

area. Consequently, the measured probe pressure  $p_{0,2}$  is higher than that which would be measured for  $A_e$ . This error tends to counterbalance the effect of neglecting the factor  $\psi(M_2)$ . Coincidentally, this is indeed the situation for thruster T-2, as the following example demonstrates.

Two data points taken at an electrical power input of 28 kilowatts for the radiation-cooled-nozzle thruster T-1 and at 28.3 kilowatts for the water-cooled-nozzle thruster T-2 will be used to evaluate the simplified probe technique used herein. The pertinent experimental data and the computed performance using both methods are presented in table II. For comparison, the calculated performance obtained from the gas power, propellant flow rate, and nozzle geometry is also given. The total-pressure ratio ( $p_{0,2}/p_{0,1}$ ) determines both the proper nozzle area ratio (or effective exit area  $A_e$  since  $A^*$  is known) and the thrust correction factor (fig. 17). A comparison of the water-cooled-nozzle specific impulses indicates that use of the correct thrust ratio (1.12) and use of a corrected exit area yield, within the experimental error, the same specific impulse obtained with the approximate equation (A6) (i.e.,  $I_{vac} = 710$  sec and  $I_{vac,cor} = 694$  sec). For the radiation-cooled nozzle, however, the corrected specific impulse changes appreciably ( $I_{vac} = 825$  sec and  $I_{vac,cor} = 768$  sec), largely as a result of the greater displacement thickness of the boundary layer on the hot nozzle wall. From these considerations, it is concluded that, when the single probe measurement is used for determining thrust, a knowledge of the effective nozzle exit area is crucial for accurate determination of thruster performance.

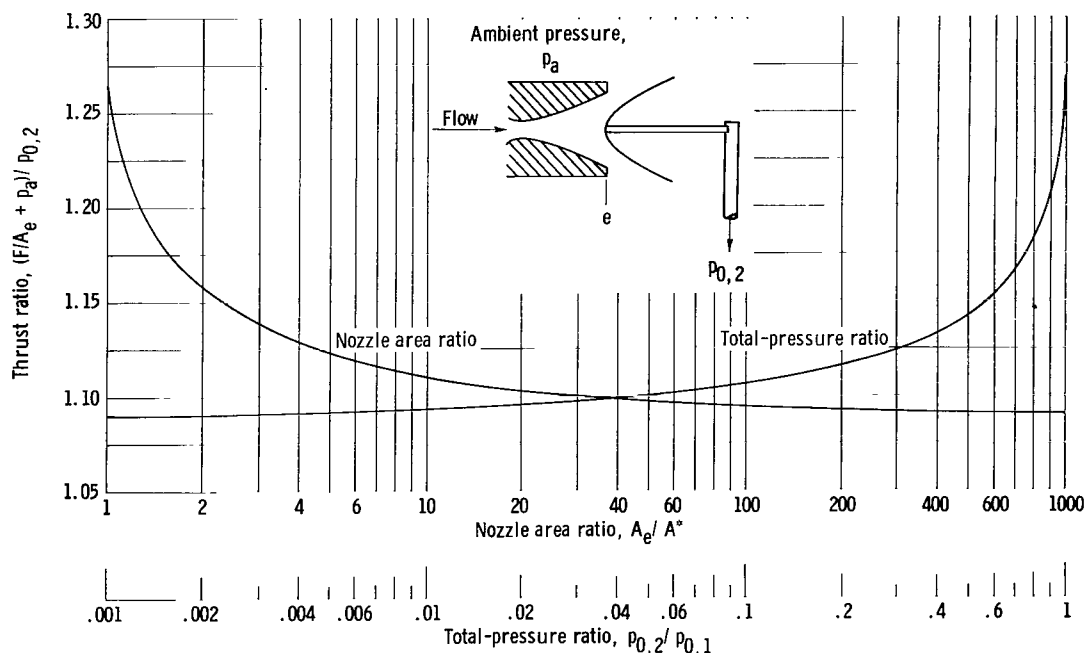


Figure 17. - Variation of thrust as a function of area ratio and pressure ratio.



TABLE II. - EXPERIMENTAL DATA AND COMPUTED PERFORMANCE FOR TWO NOZZLE CONFIGURATIONS

Thruster	Throat area, $A^*$ , sq in.	Basic data			Computed performance		
		Heating efficiency, $P_p/P_E$	Stagnation pressure, $P_{0,1}$ , lb/sq in.	Probe stagnation pressure, $P_{0,2}$ , lb/sq in.	Based on approx. eq. (A6), $I_{vac} = \frac{P_{0,2} A_e}{\dot{w}}$ , sec	Based on corrected eq. (A5), $I_{vac, cor} = \frac{P_{0,2} A_e (1 + \psi)}{\dot{w}}$ , sec	Based on gas power per unit flow rate $P_p/\dot{w}$ (fig. 10), $I_{vac}$ , sec
T-1	0.036	0.549	13.12	4.3	825	<sup>a</sup> 768	760
T-2	0.036	0.441	12.2	3.7	710	<sup>b</sup> 694	710

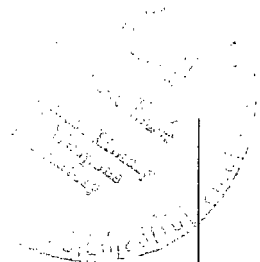
<sup>a</sup> $(A_e/A^*)_{cor} = 4.40$  and  $1 + \psi = 1.127$  (values from fig. 17) where  $\psi$  is the Mach number parameter.

<sup>b</sup> $(A_e/A^*)_{cor} = 4.63$ ;  $1 + \psi = 1.125$ .

## REFERENCES

1. Jack, J. R.: NASA Research on Resistance-Heated Hydrogen Jets. Paper Presented at AFOSR Symposium on Advanced Propulsion Concepts, Cincinnati (Ohio), Oct. 2-4, 1962.
2. Jack, John R., and Spisz, Ernie W.: NASA Research on Resistance-Heated Hydrogen Jets. Paper 63023, AIAA, 1963.
3. Jack, John R.: Theoretical Performance of Propellants Suitable for Electro-thermal Jet Engines. Preprint 1506-60, Am. Rocket Soc., Inc., 1960.
4. King, Charles R.: Compilation of Thermodynamic Properties, Transport Properties, and Theoretical Rocket Performance of Gaseous Hydrogen. NASA TN D-275, 1960.
5. Spisz, E. W.: Compilation of Theoretical Rocket Performance for the Chemically Frozen Expansion of Hydrogen. NASA TN D-2080, 1963.
6. Short, G. R., and Howard, J. M.: Sublimation of Tungsten in Hydrogen. Paper 63024, AIAA, 1963.
7. Staff of the Department of Electrical Engineering, M.I.T.: Applied Electronics. John Wiley & Sons, Inc., 1943.
8. Shapiro, Ascher H.: The Dynamics and Thermodynamics of Compressible Fluid Flow. Vol. 1. The Ronald Press Co., 1953.

2/7/25  
28



*"The National Aeronautics and Space Administration . . . shall . . . provide for the widest practical appropriate dissemination of information concerning its activities and the results thereof . . . objectives being the expansion of human knowledge of phenomena in the atmosphere and space."*

—NATIONAL AERONAUTICS AND SPACE ACT OF 1958

## NASA SCIENTIFIC AND TECHNICAL PUBLICATIONS

**TECHNICAL REPORTS:** Scientific and technical information considered important, complete, and a lasting contribution to existing knowledge.

**TECHNICAL NOTES:** Information less broad in scope but nevertheless of importance as a contribution to existing knowledge.

**TECHNICAL MEMORANDUMS:** Information receiving limited distribution because of preliminary data, security classification, or other reasons.

**CONTRACTOR REPORTS:** Technical information generated in connection with a NASA contract or grant and released under NASA auspices.

**TECHNICAL TRANSLATIONS:** Information published in a foreign language considered to merit NASA distribution in English.

**TECHNICAL REPRINTS:** Information derived from NASA activities and initially published in the form of journal articles or meeting papers.

**SPECIAL PUBLICATIONS:** Information derived from or of value to NASA activities but not necessarily reporting the results of individual NASA-programmed scientific efforts. Publications include conference proceedings, monographs, data compilations, handbooks, sourcebooks, and special bibliographies.

*Details on the availability of these publications may be obtained from:*

SCIENTIFIC AND TECHNICAL INFORMATION DIVISION  
NATIONAL AERONAUTICS AND SPACE ADMINISTRATION

Washington, D.C. 20546